FACS-purified myoblasts producing controlled VEGF levels induce safe and stable angiogenesis in chronic hind limb ischemia

Thomas Wolff [a, b], **Edin Mujagic** [a, b], **Roberto Gianni-Barrera** [a], **Philipp Fueglistaler** [a, b], **Uta Helmrich** [a], **Heidi Misteli** [a, b], **Lorenz Gurke** [b], **Michael Heberer** [a, b], **Andrea Banfi** [a, *]

[a] *Cell and Gene Therapy, Department of Biomedicine, Basel University Hospital, Basel, Switzerland*
[b] *Vascular Surgery, Department of Surgery, Basel University Hospital, Basel, Switzerland*

Abstract

We recently developed a method to control the *in vivo* distribution of vascular endothelial growth factor (VEGF) by high throughput Fluorescence-Activated Cell Sorting (FACS) purification of transduced progenitors such that they homogeneously express specific VEGF levels. Here we investigated the long-term safety of this method in chronic hind limb ischemia in nude rats. Primary myoblasts were transduced to co-express rat VEGF-A$_{164}$ (rVEGF) and truncated ratCD8a, the latter serving as a FACS-quantifiable surface marker. Based on the CD8 fluorescence of a reference clonal population, which expressed the desired VEGF level, cells producing similar VEGF levels were sorted from the primary population, which contained cells with very heterogeneous VEGF levels. One week after ischemia induction, 12×10^6 cells were implanted in the thigh muscles. Unsorted myoblasts caused angioma-like structures, whereas purified cells only induced normal capillaries that were stable after 3 months. Vessel density was doubled in engrafted areas, but only approximately 0.1% of muscle volume showed cell engraftment, explaining why no increase in total blood flow was observed. In conclusion, the use of FACS-purified myoblasts granted the cell-by-cell control of VEGF expression levels, which ensured long-term safety in a model of chronic ischemia. Based on these results, the total number of implanted cells required to achieve efficacy will need to be determined before a clinical application.

Keywords: therapeutic angiogenesis ● flow cytometry ● vascular endothelial growth factor ● chronic ischemia ● cell therapy ● gene therapy

Introduction

Therapeutic angiogenesis is the induction of new blood vessels by the delivery of specific growth factors and is a potentially powerful strategy to treat ischemic conditions. Vascular endothelial growth factor-A (VEGF-A) is the most potent and specific angiogenic factor [1]. VEGF gene therapy using naked DNA or adenoviral vectors has already been investigated in several clinical trials both for ischemic heart and peripheral artery disease. Initial results were positive, but placebo-controlled phase II studies did not confirm clinical efficacy [2]. The major obstacle appears to be the narrow therapeutic window of VEGF gene therapy, so that small increases in vector dose rapidly go from lack of efficacy to toxic effects, such as the growth of haemangiomas [3–7].

Because VEGF remains tightly bound to the extracellular matrix and does not diffuse through tissue [8], the induction of normal or aberrant angiogenesis depends on the level of VEGF expression in the microenvironment around each producing cell, and not on the total dose delivered [9, 10]. Using retrovirally transduced myoblasts with stable VEGF expression in skeletal muscle, we could previously show that even small numbers of cells expressing high VEGF levels within a heterogeneous population always caused angioma growth. However, when homogeneous expression was achieved by implanting clonal populations, in which every cell produced the same amount, a dose-dependent effect of VEGF became apparent, where a wide range of levels induced only normal, stable and functional vessels, whereas angioma growth occurred above a defined threshold level [9]. Although the use of

*Correspondence to: Dr. Andrea BANFI,
Cell and Gene Therapy, Basel University Hospital,
ICFS 407, Hebelstrasse 20,
Basel CH-4031, Switzerland.
Tel.: +41-61-265 3507
Fax: +41-61-265 3990
E-mail: abanfi@uhbs.ch

clonal populations clearly demonstrated the need to control VEGF expression at the microenvironmental level, this approach is unsuitable for a clinical application, because it requires extensive *in vitro* expansion of the transduced myoblasts, making it very time consuming and costly. We therefore developed a high-throughput FACS-based method to rapidly isolate the cells expressing a specific VEGF level from a heterogeneous population of transduced progenitors. We have recently shown that a single round of FACS sorting provided populations of VEGF-expressing myoblasts, which avoided any angioma growth and induced robust normal angiogenesis in non-ischemic tissue. The angiogenic effect was equivalent to clonal populations expressing similar VEGF levels, but with the critical advantage that a large number of cells were generated rapidly [11].

These results were obtained in non-ischemic skeletal muscle. However, in ischemic tissue a variety of endogenous angiogenic pathways are up-regulated and might alter the effects of exogenously delivered growth factors. In this study we investigated, whether long-term controlled VEGF expression by FACS-purified myoblasts could induce safe angiogenesis and prevent aberrant vascular growth in a rat model of chronic hind limb ischemia.

Materials and methods

Retrovirus production

A truncated version of the rat CD8a gene (tr.rCD8a) was generated by PCR from the full-length transcript (NCBI accession number NM_031538). Primers were designed to amplify a fragment of rat CD8a spanning codons 1–222, including the signal peptide, the full extracellular and transmembrane regions, and truncating the cytoplasmic region after the first five amino acids (218–222): CD8-FW: 5′-CAC ACC ATG GCC TCA CGG GTG ATC TGC-3′, CD8-RV: 5′-AAA CGC TAG CTT AGT TCC TGT GGC AGC AG-3′. The full coding sequence of rat VEGF$_{164}$ (NCBI accession number NM_031836) was amplified using the following primers: VEGF-FW: 5′-ACG CGT ATG AAC TTT CTG CTC TCT TGG GTG C-3′, VEGF-RV: 5′-TTT TGC GGC CGC TCA CCG CCT TGG CTT-3′. Total RNA was extracted from rat thymus and kidney using an RNeasy kit (QIAgen, Basel, Switzerland). After retro transcription of 1 μg of RNA, the tr.rCD8a fragment and the rat VEGF$_{164}$ cDNA were generated by PCR according to these conditions: 94°C × 2′ + (94°C × 30″ + 55°C × 30″ + 68°C × 1′) × 40 cycles + 68°C × 7′. The retroviral construct was generated by cloning the cDNAs encoding rVEGF and tr.rCD8a upstream and downstream of an encephalomyocarditis virus internal ribosomal entry sequence (IRES), under the control of the retroviral promoter, in order to allow the translation of both sequences from a single transcript [12].

Cell culture

Primary myoblasts isolated from C57BL/6 mice and transduced to express the β-galactosidase marker gene (lacZ) from a retroviral promoter [13] were further transduced at high efficiency with the pAMFG-rVICD8 retrovirus through four rounds of infection, according to a previously published protocol [14]. Negative control cells (rICD8) were produced with a

similar retrovirus that expressed tr.rCD8 but no VEGF. Early passage myoblast clones homogeneously expressing specific levels of VEGF and tr.rCD8a were isolated using a FACS Vantage SE cell sorter (Becton Dickinson, Basel, Switzerland) as previously described [9] and single cell isolation was confirmed visually. All myoblast populations were cultured in 5% CO_2 on collagen-coated dishes, with a growth medium consisting of 40% F10, 40% low-glucose DMEM and 20% foetal bovine serum, supplemented with 2.5 ng/ml basic fibroblast growth factor-2, as previously described [15].

VEGF$_{164}$ ELISA measurements

The production of VEGF-A$_{164}$ in cell culture supernatants was quantified using a Quantikine rat VEGF Immunoassay ELISA kit (R&D Systems Europe, Abingdon, UK). One millilitre of medium was harvested from myoblasts cultured in a 60 mm dish, following 4 hrs of incubation, then filtered and analysed in duplicate. Results were normalized by the number of cells and time of incubation. Four separate dishes of cells were assayed for each cell type ($n = 4$).

CD8a detection by FACS

Expression of tr.rCD8a by individual cells was assessed by staining transduced myoblasts with a specific mouse monoclonal antibody to rat CD8a directly conjugated to Fluorescein Isothiocyanate (FITC, clone OX-8; BD Biosciences, Basel, Switzerland). Cells were stained for 20 min. on ice with a solution containing 2 μg of antibody in 200 μl of 5% bovine serum albumin (BSA) in PBS for every 10^6 cells. Preliminary experiments determined that these staining conditions ensured complete saturation of the tr.rCD8a molecules expressed on all cells of the primary transduced population. Data were acquired with a FACSCalibur flow cytometer (Becton Dickinson) and analysed using FlowJo software (Tree Star, Ashland, OR, USA). Mean fluorescence intensity was used to quantify the tr.rCD8a expression.

Myoblast injection in SCID mice

For the evaluation of angiogenesis in non-ischemic tissue, cells were implanted into 6–8-week-old Severe Combined ImmunoDeficiency (SCID) CB.17 mice (Charles River Laboratories, Sulzfeld, Germany) in order to avoid an immunological response to β-galactosidase- and rat VEGF-expressing myoblasts. Animals were treated in accordance with Swiss Federal guidelines for animal welfare and the study protocol was approved by the Veterinary Office of the Canton Basel-Stadt (Basel, Switzerland). Myoblasts were dissociated in trypsin and resuspended in PBS with 0.5% BSA. 500,000 myoblasts in 5 μl were implanted into the posterior auricular muscle, midway up the dorsal aspect of the external ear, using a syringe with a 29^1/$_2$G needle.

Surgical induction of chronic hind limb ischemia in the rat

In order to avoid an immunological response to mouse myoblasts, NIH-*Foxn1^{rnu}* nude rats aged 9–11 weeks (Charles River Laboratories) were used. Rats were randomized before surgery to receive either vehicle only or

one of the four cell populations. The animals underwent bilateral excision of a femoral artery segment under 2% isoflurane anaesthesia, as previously described [16, 17]. Briefly, the femoral artery was prepared as close as possible to the inguinal ligament, tied with prolene 6-0 sutures, taking care not to injure the femoral nerve, and a 3 mm segment of the artery was excised. One week later the skin incision was reopened under isoflurane anaesthesia and the surface of the medial thigh and quadriceps muscles were exposed. Myoblasts were suspended at a concentration of 100,000 cells/μl and 10 μl (1 million cells) per site were injected at 12 defined locations in the medial hamstring and quadriceps muscles using a $29^{1}/_{2}$G needle.

Blood flow determination

Regional blood flow in the hind limb was determined by radioactive microsphere injection, as previously described [16, 18]. Briefly, on the day of blood flow measurement a 0.965 mm polyethylene catheter (PE 50, Becton Dickinson) was placed in the aortic arch *via* the left carotid artery for microsphere injection and another catheter was placed in the caudal artery for withdrawal of the reference blood sample. Both catheters were subcutaneously tunnelled to the back of the neck, flushed with heparinized saline and incisions were closed. Animals were allowed to recover for approximately 4 hrs, after which blood flow measurements were performed while the animal was running on a treadmill (15% slope). Two measurements were performed with microspheres labelled with different isotopes, while the animals were running at two different speeds. Flow at the two different speeds did not differ, showing that blood flow was limited by the maximal collateral conductance and not by muscle metabolic demand. Approximately 1 million ^{141}Ce-labelled 15 μm microspheres (PerkinElmer, Waltham, MA, USA) were continuously injected into the aortic arch over 20 sec., starting 60 sec. after the animal had begun running at 20 cm/sec. Withdrawal of reference blood from the caudal artery at a rate of precisely 0.5 ml/min. was begun 10 sec. before initiation of injection and continued for approximately 90 sec. After microsphere delivery, the aortic catheter was flushed with saline. Rats were then allowed to rest for approximately 5 min. and recovery of blood pressure and heart rate to base line values was confirmed. The procedure was then repeated with the rat running at 30 cm/sec., injecting ^{85}Sr-labelled microspheres. After the second microsphere injection, the animals were killed with an intravenous pentobarbital injection and tissues were dissected from both hind limbs. The quadriceps, medial hamstring and gastrocnemius muscles were harvested separately and weighed. Radioactivity was measured on a gamma counter along with the reference blood sample, yielding the counts per minute (CPM) of each sample. Absolute blood flow in ml/min./100 g tissue was then calculated according to the formula $CPM_{tissue}/blood\ flow_{tissue} = CPM_{reference\ blood}/withdrawal\ rate$. The average of the blood flow measurements from the corresponding right and left muscles determined at the higher running speed was taken as maximum blood flow.

Tissue staining

The entire vascular network of the ear could be visualized after intravascular staining with a biotinylated *Lycopersicon esculentum* (tomato) lectin (Vector Laboratories, Burlingame, CA, USA) that binds the luminal surface of all blood vessels, as previously described [9]. Briefly, mice were anesthetized, lectin was injected intravenously and 4 min. later the tissues were fixed by vascular perfusion of 1% paraformaldehyde and 0.5% glutaraldehyde in PBS, pH 7.4 at 120 mmHg of pressure. Ears were then removed, bisected in the plane of the cartilage, and stained with X-gal staining buffer

(1 mg/ml 5-bromo-4-chloro-3-indoyl-b-D-galactoside, 5 mM potassium ferricyanide, 5 mM potassium ferrocyanide, 0.02% Nonidet P-40, 0.01% sodium deoxycholate, 1 mM MgCl$_2$, in PBS, pH 7.4). Lectin-coated vessels were stained using avidin–biotin complex-diaminobenzidine histochemistry (Vector Laboratories), dehydrated through an alcohol series, cleared with toluene and whole-mounted on glass slides with Permount embedding medium (Fisher Scientific, Wohlen, Switzerland). Vascular morphology was analysed 4 weeks after myoblast implantation.

To obtain rat muscle sections, the animals were anesthetized by intraperitoneal pentobarbital and tissues were fixed by vascular perfusion *via* a cannula in the left ventricle with 200 ml of 1% paraformaldehyde in PBS, pH 7.4. The medial hamstring muscle (largest muscle of the adductor muscle group) was harvested in one piece, embedded in OCT compound (Sakura Finetek, Torrance, CA, USA), frozen in freezing isopentane and the entire muscle was cryosectioned. Tissue sections were then stained with X-gal (20 μm sections) or with haematoxylin and eosin (10 μm sections) as described previously [13]. Immunofluorescence on 10 μm sections was performed as previously described [9]. The following primary antibodies and dilutions used were: mouse monoclonal anti-rat Platelet-Endothelial Cell Adhesion Molecule-1 (PECAM-1, Clone TLD-3A12; AbD Serotec, Düsseldorf, Germany) at 1:100; mouse monoclonal anti-α-SMA (Clone 1A4; MP Biomedicals, Basel, Switzerland) at 1:400; rabbit polyclonal anti-Nerve/Glial antigen-2 (NG2; Chemicon Europe, Chandlers Ford, UK) at 1:200. Fluorescently labelled secondary antibodies (Invitrogen, Basel, Switzerland) were used at 1:200.

Vessel measurements

Regions of myoblast engraftment were determined by identifying β-galactosidase^{+} muscle fibres on X-Gal stained sections. The corresponding regions were then identified on immunostained sections and images were taken with a 20$\times$ objective on an Olympus BX61 microscope (Münster, Germany). Five images were acquired for each condition. Vessel centrelines were manually traced, quantified using the AnalySIS D software (Soft Imaging System Gmbh, Münster, Germany) and normalized to the number of muscle fibres. Vessel length density (VLD) was expressed in micrometre of vessel length/fibre. The extent of myoblast engraftment was quantified by analysing the entire treated adductor muscles sectioned at 0.5 mm intervals and measuring the area of β-galactosidase^{+} muscle fibres in relation to the area of the entire section on low magnification images using ImageJ software. This allowed us to estimate myoblast engraftment as a percentage of total muscle volume.

Statistics

Data are presented as means $\pm$ S.E. The significance of differences was evaluated using ANOVA followed by the Bonferroni test (for multiple comparisons), or using a Student's t-test (for pair wise comparisons). $P < 0.05$ was considered statistically significant.

Results

Generation of rVICD8 myoblasts

Nude rats lack T-cell-based immunity, but have an intact capacity to generate antibodies. In order to avoid a humoral response
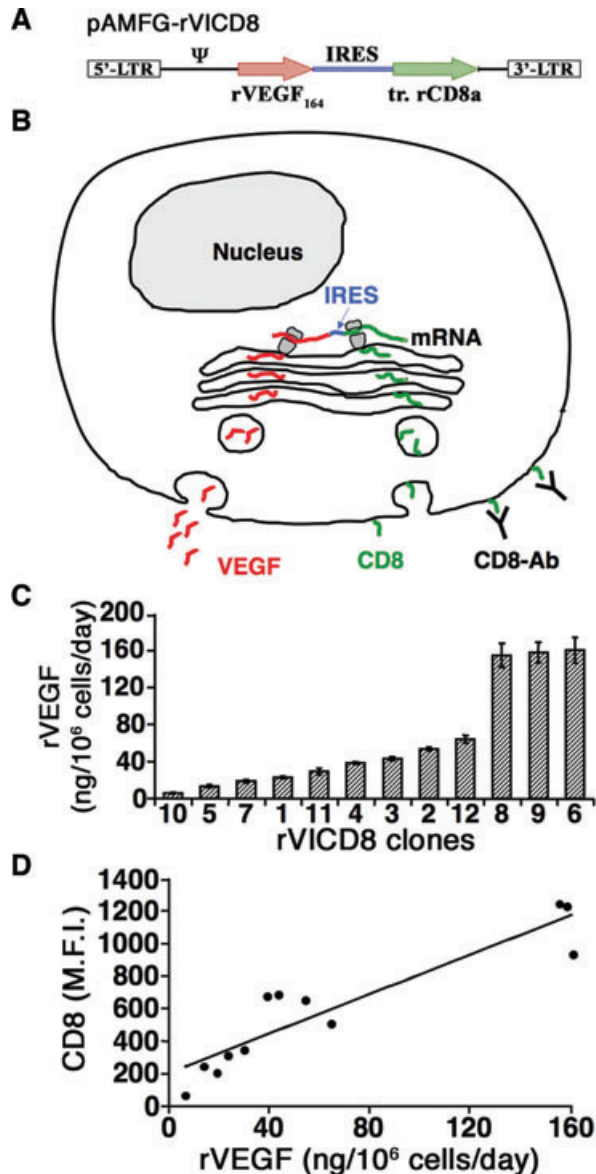
Fig. 1 rCD8a expression correlates linearly with rVEGF production in rVICD8 myoblasts. (**A**) The coding sequences for rat VEGF164 (rVEGF164) and truncated rat CD8a (tr. rCD8a) were linked through an Internal Ribosomal Entry Site (IRES) sequence in a bicistronic retroviral construct (pAMFG-rVICD8). ψ: retroviral packaging signal; LTR: long terminal repeats. (**B**) Schematic representation showing co-expression of both genes at a fixed ratio from the bicistronic mRNA, so that the amount of VEGF secreted (red molecules) is correlated to that of tr.rCD8a retained on the cell surface (green molecules), which can be quantified by staining with an anti-rCD8a antibody (CD8-Ab). (**C**) The production of rVEGF (in ng/106 cells/day) was measured by ELISA in supernatants of 12 individual myoblast clones isolated from the primary transduced rVICD8 population (n = 3–5). (**D**) Correlation between the expression of rCD8a, quantified by FACS, and the amount of secreted rVEGF, quantified by ELISA, in the 12 clonal populations analyzed. MFI: mean fluorescence intensity.

against xenogenic VEGF, we therefore generated a population of primary myoblasts that stably expressed rVEGF and adapted the FACS-purification technology recently described for murine VEGF to rVEGF. A bicistronic retroviral vector (pAMFG-rVICD8, Fig. 1A; rVICD8 = rat Vegf-Ires-CD8) was constructed carrying the cDNA for rVEGF and tr.rCD8a joined through an internal ribosomal entry site [12]. Both coding sequences are thus transcribed from a single mRNA molecule under the control of the same promoter and co-expressed at fixed relative levels [19]. With this configuration, the quantity of tr.rCD8a accumulated on the cell surface, which can be measured by FACS after staining with a specific antibody, should correlate with the amount of rVEGF secreted by each cell (Fig. 1B). To verify this hypothesis, primary mouse myoblasts, which already expressed LacZ from a different retroviral construct [13], were stably transduced with the rVICD8 vector with greater than 99% efficiency. Thirty-three clones were randomly isolated from the primary transduced cell population and expanded. They secreted a wide range of VEGF levels, showing that the expression levels in the primary transduced population were in fact very heterogeneous. From these 33 clones we selected 12 that produced less than 200 ng of rVEGF/10^6 cells/day for further analysis (range of VEGF levels from 5.6 ± 0.7 to 160.4 ± 13.9 ng/10^6 cells/day, Fig. 1C). The expression of tr.rCD8a in these clones was quantified by FACS after staining under optimized conditions. The expression of tr.rCD8a displayed a good overall correlation with *in vitro* rVEGF production (R^2 = 0.85, Fig. 1D).

FACS sorting for homogeneous VEGF expression

To determine the angiogenic response to specific rVEGF levels *in vivo*, seven of the clones were injected into auricularis muscles of SCID mice (n = 6 per condition) and compared to the unsorted transduced population and to negative control cells expressing only tr.rCD8a (rCD8 cells). Four weeks after implantation, the four clones with VEGF levels less than 60 ng/10^6 cells/day had a clear angiogenic effect compared to rCD8 cells (Fig. 2A) and induced only homogeneous, normal capillaries (*e.g.* clone 2, Fig. 2C). The three clones with VEGF levels of 140–150 ng/10^6 cells/day always induced the growth of aberrant, angioma-like vascular structures (*e.g.* clone 8, Fig. 2D), similar to those caused by the unsorted population (Fig. 2B). On the basis of these results, clone 2, which produced 53.5 ± 2.1 ng of rVEGF/10^6 cells/day and induced normal angiogenesis, was chosen to provide the reference values for the definition of the sorting gate, by which FACS purification could be performed. The FACS gate was designed to represent the middle 25% of the range of fluorescence intensity values on the reference population's histogram plot, as shown in Figure 2E. This gate size was chosen because we previously found that less restrictive gates can lead to a small contamination with cells expressing higher levels than expected [11]. The gate was applied to the heterogeneous primary transduced population. Re-analysis immediately after the sorting showed that the rCD8 expression of the purified population was completely contained within the gate (blue curve in Fig. 2F).
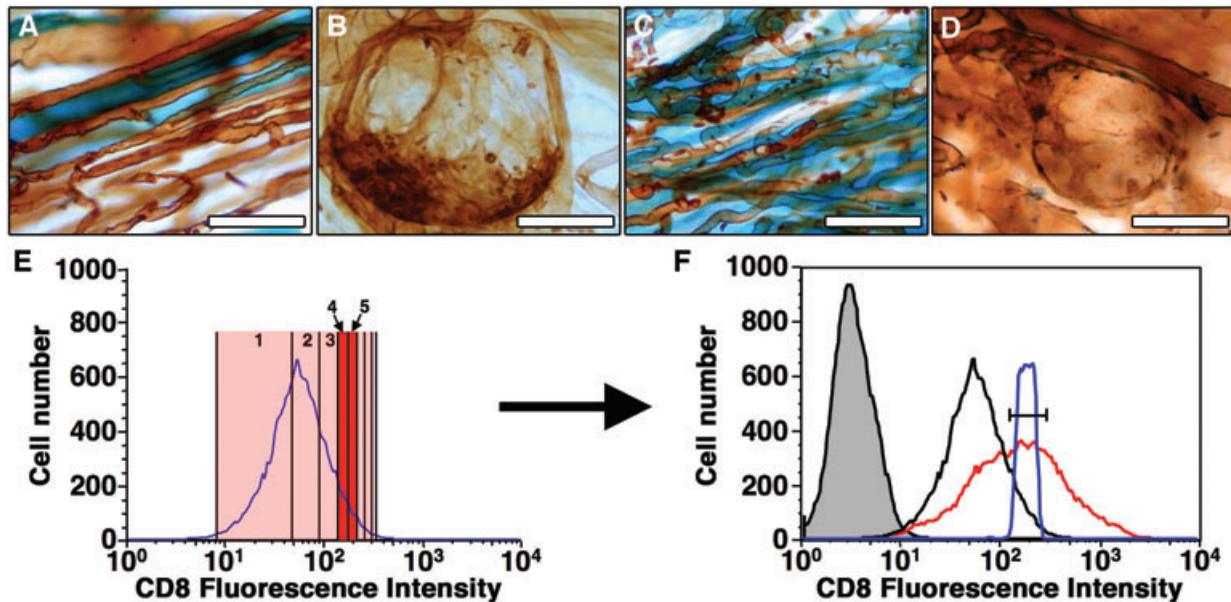
Fig. 2: FACS-purification yields a myoblast population expressing a defined rVEGF level. Control rICD8 cells (**A**), primary transduced rVICD8 myoblasts (**B**) and clones expressing moderate (**C**, clone 2) or high VEGF levels (**D**, clone 8) were implanted in the posterior auricularis muscle of SCID mice. Four weeks later, vascular morphology was analszed in tissue whole-mounts by lectin staining (brown) and myoblast engraftment was revealed by X-Gal staining (blue). Size bars = 50 μm. (**E**) Clone 2, producing 53.5 $\pm$ 2.1 ng of rVEGF/10^6 cells/day, was chosen as the reference clone. Its range of fluorescence intensity (pink shade) was divided into eight equal parts, shown by the vertical lines on the logarithmic scale of the FACS plot, and the middle two octiles (25%) defined the sorting gate (red shade). (**F**) This gate (black segment bar) was applied to the heterogeneous rVICD8 population (red curve) to yield the purified population (blue curve). The reference clone (black curve) and the negative control cells (grey-tinted curve) are also shown.

Chronic hind limb ischemia

Bilateral ligation of the femoral artery was performed in nude rats as depicted in Figure 3A. In order to confirm that induced ischemia was chronic, maximum blood flow in the thigh and calf muscles of non-treated animals were measured before ligation and at 1 and 5 weeks after ligation. No animals developed toe or foot necrosis. Maximum blood flow in the quadriceps muscle was reduced from 181 $\pm$ 11 to 141 $\pm$ 14 ml/min./100 g and remained at 137 $\pm$ 11 ml/min./100 g after 5 weeks ($P < 0.05$, Fig. 3B). Similarly, maximum blood flow in the medial hamstring muscle was reduced from 124 $\pm$ 9 to 82 $\pm$ 10 ml/min./100 g and 87 $\pm$ 8 ml/min./100 g at 1 and 5 weeks, respectively ($P < 0.01$ and $P < 0.05$, Fig. 3C). Maximum blood flow in the gastrocnemius muscle was even more drastically reduced from 176 $\pm$ 9 to 39 $\pm$ 5 ml/min./100 g 1 week after ligation and recovered slightly to 73 $\pm$ 5 ml/min./100 g after 5 weeks ($P < 0.001$ for both conditions, Fig. 3D). These results prove that bilateral ligation of the femoral artery in the nude rat leads to a persistent blood flow reduction both in the thigh and calf muscles.

Controlled angiogenesis by purified VEGF-expressing myoblasts

The different myoblast populations were implanted in 12 defined sites in the quadriceps and medial hamstring muscles 1 week after ligation, as shown graphically in Figure 3A. Control rCD8 cells produced only background rVEGF levels (0.5 $\pm$ 0.05 ng/10^6 cells/day). The average rVEGF production by the unsorted rVICD8 population was 132.1 $\pm$ 6.0 ng/10^6 cells/day, whereas the reference clone and the sorted population expressed 53.5 $\pm$ 2.1 and 37.8 $\pm$ 1.0 ng of rVEGF/10^6 cells/day, respectively. In order to assess the long-term safety of controlled VEGF expression in chronically ischemic tissue, vascular morphology and VLD were analysed histologically 3 months after cell injection in the medial hamstring muscles ($n = 4$ per condition), so as to evaluate both the stability of newly induced vessels and the possible evolution of slow-growing aberrant structures. Areas containing engrafted transduced myoblasts were visualized on X-Gal stained sections so they could be identified in the immunostained adjacent serial sections. The angiogenic effects described below were in all cases
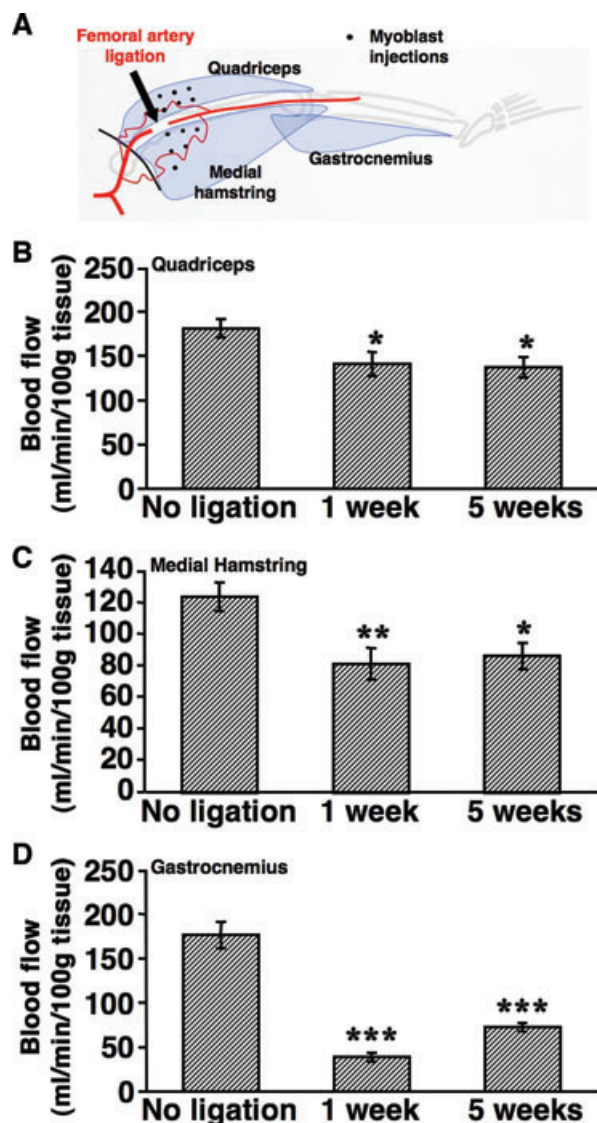
Fig. 3 Chronic hind limb ischemia model. (**A**) Schematic representation showing the location of femoral artery ligation and the 12 defined areas where myoblast populations were injected 1 week later (black dots) in the quadriceps and medial hamstring muscles. Maximum blood flow was measured in quadriceps (**B**), medial hamstring (**C**) and gastrocnemius (**D**) muscles 1 and 5 weeks after ischemia induction and in non-ligated animals. Values represent the mean $\pm$ S.E.M. ($n = 10$–12 per group). $^*P < 0.05$; $^{**}P < 0.01$; $^{***}P < 0.001$, compared to the no-ligation condition.

with NG2$^+$, SMA$^-$ pericytes (Fig. 4C). Animals treated with unsorted cells, on the other hand, showed both areas of normal angiogenesis and aberrant angioma-like vascular structures, which lacked pericytes but were covered with a thick smooth muscle layer (Fig. 4D), as to be expected with the expression of heterogeneous VEGF levels. However, implantation of the purified population completely avoided the appearance of aberrant angiogenesis and in all animals induced only normal, pericyte-covered mature capillaries (Fig. 4E). The induced normal capillaries were all mature and associated with NG2$^+$ pericytes and morphologically indistinguishable from the pre-existing microvessels in non-ischemic or control-treated muscles, regardless of which VEGF-expressing population had induced them. Only the angioma-like structures induced by unsorted cells displayed an aberrant smooth muscle coverage. The angiogenic effect of the different populations was quantified by measuring the VLD in the areas of myoblast engraftment. As shown in Figure 4F, VLD was significantly greater in animals treated with the VEGF-expressing myoblasts compared to control rCD8 cells or to non-ischemic muscle ($P < 0.05$ for all comparisons). These results show that controlled VEGF expression from FACS-purified cells in a model of chronic hind limb ischemia induced normal angiogenesis as efficiently as a clonal population with homogeneous expression of a similar VEGF level, leading to a greater than 50% increase in VLD compared to normal muscle. Both populations completely avoided the formation of aberrant vessels that were induced by the primary unsorted population.

Muscle blood flow after implantation of VEGF-expressing myoblasts

To assess whether the increased number of blood vessels in areas of engraftment of VEGF-expressing myoblasts was associated with a functional effect, maximum blood flow was measured in the thigh muscles, where cells had been injected, and further distally in the calf muscles 4 weeks after treatment, *i.e.* 5 weeks after femoral artery ligation. As shown in Figure 5, none of the populations of VEGF-expressing myoblasts significantly increased maximum blood flow in comparison to animals treated with BSA or control rCD8 cells, either in thigh or calf muscles.

Efficiency of engraftment of injected myoblasts

In order to investigate why the angiogenic induction observed by histological analysis was not accompanied by an increase in muscle blood flow, we examined the extent of stable engraftment of transduced myoblasts in the medial hamstring muscles 3 months after injection ($n = 4$ per condition). As can be seen in Figure 6A, X-Gal$^+$ muscle fibres could only be found along the needle tract of the intramuscular injections (white arrows). The engraftment pattern was similar for the control rCD8 cells, the reference clone, the primary rVICD8 population and the purified population (Fig. 6B–E,
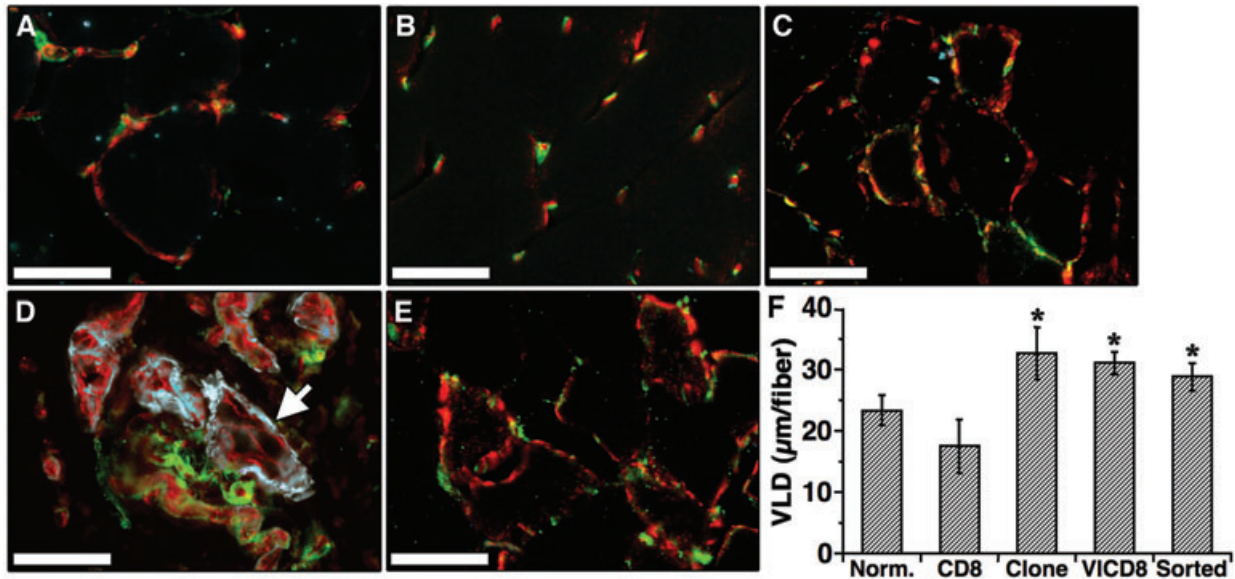
observed exclusively around transduced fibres and no effect could be found outside of these areas, which is consistent with secreted VEGF remaining localized in tissue. The vasculature in ischemic muscle treated with control rCD8 cells (Fig. 4B) was similar to that in non-ischemic, non-treated muscles (Fig. 4A). The reference clone induced the growth of normal, mature capillaries, associated

Fig. 4 FACS-purified rVICD8 myoblasts induce normal, stable and mature angiogenesis in ischemic muscle. (**A–E**) The medial hamstring muscles were harvested 3 months after myoblast injection and frozen sections were immunostained with antibodies against endothelium (PECAM, in red), pericytes (NG2, in green) and smooth muscle cells (α-SMA, in blue). Images were taken in areas where myoblast engraftment had been confirmed in adjacent serial sections stained with X-Gal. (**A**) nonischemic, non-treated muscle. (**B**) rICD8 control cells. (**C**) reference clone. (**D**) primary transduced rVICD8 population. (**E**) FACS-purified rVICD8 myoblasts. The white arrow in (**D**) indicates a large angioma-like aberrant structure. Size bars = 50 7 μm. (**F**) Vessel length density (VLD) was measured around engrafted fibres and is expressed as the mean vessel length (in μm) per fibre. Values represent the mean ± S.E.M. (n = 3–5). CD8: control cells; VICD8: primary transduced rVICD8 myoblasts. *$P < 0.05$ compared to control cells.

respectively) and in all cases accounted for only approximately 0.1–0.2% of the total volume of the treated muscle (Fig. 6F).

Discussion

VEGF is a fundamental regulator of angiogenesis both in development and disease and VEGF alone is capable of starting the complex cascade of events leading to the generation, growth and stabilization of new vessels [1], making it a very attractive candidate for the induction of therapeutic angiogenesis. However, direct gene therapy approaches have failed to establish a clear benefit in clinical trials, partly due to difficulties in establishing a therapeutic window for VEGF expression (reviewed in [2]). Prolonged expression of high VEGF levels is known to have toxic effects, such as uncontrolled vascular proliferation and the growth of angioma-like vascular tumours [4–7]. Furthermore, VEGF expression must also be sustained for at least 4 weeks to allow proper maturation of the new vessels and shorter durations lead to vascular regression [9, 20]. On the other hand, vessels that have not regressed by 4 weeks have been shown to persist for at least several months and even more than a year [9, 10, 20].

We have previously found that, in order to avoid the growth of aberrant vessels, VEGF expression must be controlled in the microenvironment around each producing cell [9], because VEGF is bound to extracellular matrix and thus tissue levels in neighbouring areas do not equilibrate. Clonal populations of transduced VEGF-producing progenitors with clearly defined VEGF secretion levels, an approach which combines the advantages of both gene therapy and cell therapy, make it possible to control microenvironmental VEGF levels while providing prolonged VEGF delivery, although this procedure is too complex to be used as a patient treatment. The technique of FACS purification offers a way to rapidly isolate myoblasts expressing safe VEGF levels with a sufficiently high throughput to be potentially useful in a clinical setting. We were previously able to show in non-ischemic tissue that FACS-purified VEGF secreting myoblasts had comparable angiogenic effects as clonal myoblast populations with corresponding VEGF levels, while also avoiding the growth of aberrant vessels and vascular tumours [11]. The data presented here show that this approach both induces robust angiogenesis and is safe in the long term when applied in a model of chronic hind limb ischemia. Stable, normal and mature vessels were induced, whereas aberrant angioma-like structures, which were invariably caused by uncontrolled VEGF expression, were completely avoided. Investigating angiogenic strategies in ischemia models is crucial, as endogenous angiogenic pathways may be up-regulated in ischemia, potentially rendering strategies unsafe, that previously had proved safe in non-ischemic tissue.
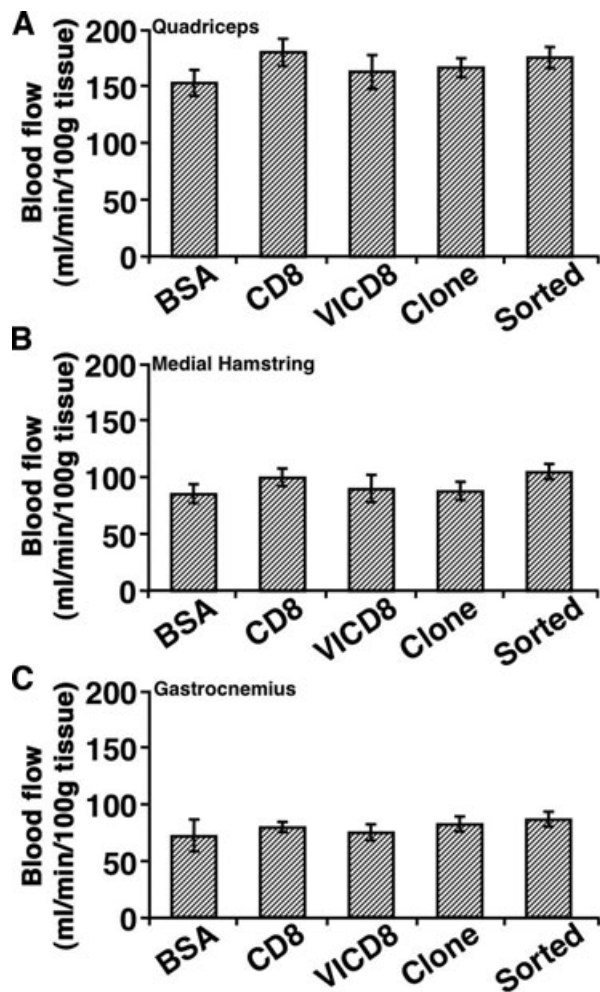
Fig. 5 Blood flow is not increased by implantation of VEGF-expressing myoblasts. Maximum blood flow in the quadriceps (**A**), the medial hamstring (**B**) and the gastrocnemius (**C**) muscle groups was measured 4 weeks after treatment (5 weeks after ligation). CD8: control cells; VICD8: primary transduced rVICD8 myoblasts. Values represent the mean ± S.E.M. ($n = 10$–12).

However, although the induction of angiogenesis was robust at the microenvironmental level, causing approximately a doubling of VLD around the fibres where myoblasts had engrafted, it did not improve global muscle blood flow, neither in the injected muscles nor further distally. This divergence between morphological and functional effects was not due to the VEGF dose, but can be explained by the fact that the delivered myoblasts had engrafted only in less than 0.2% of the total volume of treated muscles, in fibres around the injection needle tracts. The angiogenic effect was thus restricted to a minimal portion of the treated muscle. It is not likely that human myoblasts would prove to have a significantly different engraftment rate. In fact, in clinical trials of myoblast transplantation for Duchenne muscular dystrophy,
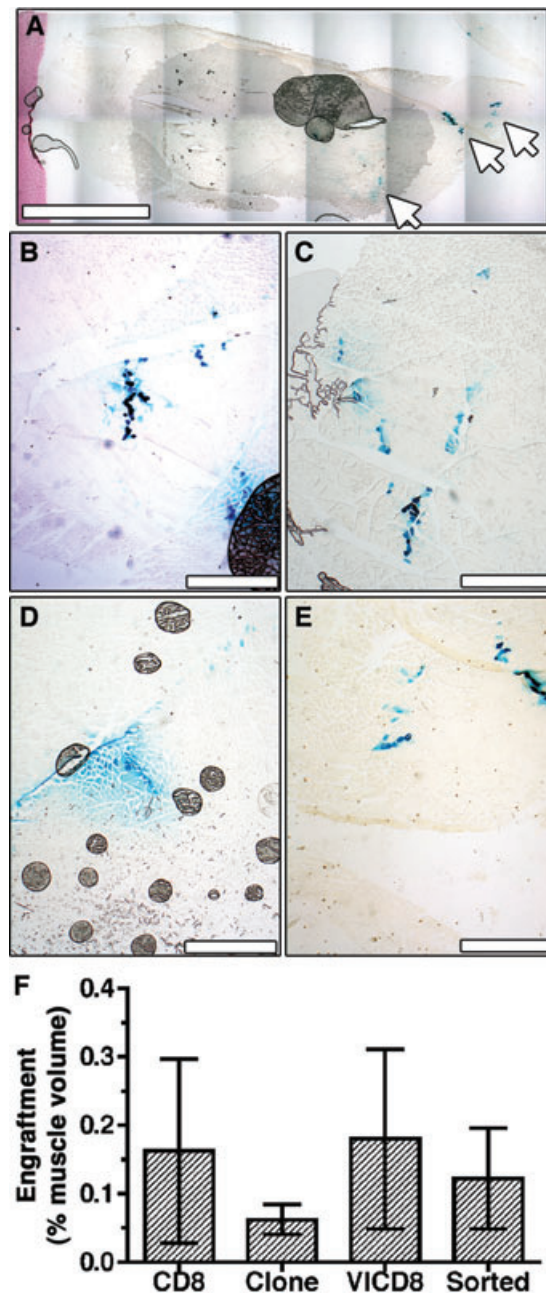

Fig. 6 Myoblast engraftment is minimal compared to muscle size. Myoblast engraftment was revealed by X-Gal staining (blue) on frozen sections of the same medial hamstring muscles shown in Figure 4. (**A**) A low magnification image of a cross-section of the entire muscle implanted with transduced myoblasts shows cell engraftment only along the needle tracts of cell injections (white arrows). Higher magnification images showing similarly low engraftment rates with control cells (**B**), reference clone cells (**C**), the primary transduced population (**D**) and purified cells (**E**). Size bars = 4 mm (**A**) and 400 μm (**B**–**E**). (**F**) Engraftment was quantified on all X-Gal stained sections and expressed as a percent of the total muscle volume ($n = 3$–5).

only about 10% of the donor myoblasts successfully engrafted in the recipient muscles [21].

These results have important implications for the planning of clinical strategies of VEGF delivery for therapeutic angiogenesis and highlight the importance of controlling dose both at the microenvironmental and at the global level. Control of the microenvironmental dose is crucial to ensure safety, as a limited number of cells with high VEGF expression can cause vascular tumours [9]. On the other hand, for efficacy the correct microenvironmental level must be achieved in a large enough volume of the target tissue, in order to induce a sufficient number of vessels and significantly affect tissue blood flow. In fact, intramuscular delivery, as opposed to intravascular perfusion methods, leads to VEGF accumulation only at the site of microvascular capillary networks, whereas collateral arteries, which need to be remodelled by the process of arteriogenesis in order to efficiently restore global blood flow, are located at anatomically remote sites and cannot be directly affected by the expressed factor [22]. However, we have previously found that sufficient stimulation of microvascular angiogenesis in ischemic skeletal muscle, through controlled VEGF expression by clonal populations of transduced myoblasts, can efficiently induce collateral arteriogenesis in a remote muscle group [10]. The increased microcirculation may activate collateral growth through increased fluid shear stress, which has been shown to potently drive arteriogenesis through a nitric oxide-dependent mechanism [23].

It has been recognized that the complexity of growth factor dosing may be pivotal for the lack of efficacy in VEGF gene therapy clinical trials [24] and it has been advocated that preclinical development of vectors should include the routine analysis of 'STED' parameters: (*i*) spread through the tissue; (*ii*) transfection efficiency; (*iii*) expression strength and (*iv*) duration of expression [25]. Within this framework, our data show that FACS purification of stably transduced myoblasts provides a high-throughput method to precisely control the distribution of microenvironmental expression levels (accounting for parameters T and E) for a sufficient duration to allow vessel stabilization (parameter D) in ischemic tissue. Specific studies are now needed to determine the number of cells and the implantation technique necessary to also achieve functional improvement (parameter S). It can however be said that the use of FACS-purified myoblasts is unique because it makes it possible to independently control the level of expression in the microenvironment (defined by the sorting parameters) and the total delivered dose (defined by the number of implanted cells).

Interestingly, recently published results by Kupatt *et al.* [26] suggest that the efficacy of VEGF-induced angiogenesis could be improved by Plateled-Derived Growth Factor-BB (PDGF-BB) co-delivery, leading to increased arteriogenesis at vector doses that were inefficient with VEGF alone, highlighting the fact that not only the kinetics of an individual growth factor but also the interplay between different growth factors is of great importance.

To induce chronic hind limb ischemia, we employed a previously described model of bilateral ligation of the femoral artery in the rat [16, 17], in which no spontaneous recovery in blood flow

was observed over at least 5 weeks. This leads to a moderate state of ischemia, whereby blood flow at rest is sufficient to prevent tissue necrosis, but maximum blood flow is drastically reduced during exercise, mimicking the clinical situation of a claudicant patient with ischemic leg pain on exercise. The model reflects the clinical situation of a large number of peripheral artery disease patients that are candidates for therapeutic angiogenesis interventions. Tissue blood flow was measured by radio-labelled microsphere injection, which is the gold standard for regional blood flow measurement. In fact, it is the only method that yields absolute values of blood flow for inter-individual comparisons and truly measures whole-muscle flow, rather than superficial perfusion in the skin, as with Doppler-based methods [27].

In a potential clinical application autologous myoblasts, cultured from a muscle biopsy, would be transduced, FACS-purified and transplanted back into the patient. To evaluate the entire procedure in a rat model of chronic ischemia it would be preferable to use autologous rat myoblasts. However, primary rat myoblasts could not be significantly expanded after isolation, both by us (Fueglistaler and Banfi, unpublished results) and others [28], as they rapidly lose their myogenic potential during *in vitro* culture. For the present experiments we thus needed to use primary mouse myoblasts, which were transduced to express rat VEGF and CD8 and implanted them in nude rats. However, it should be noted that human myoblasts can be easily expanded *in vitro* without loss of differentiation potential and large numbers of cells have been routinely generated to treat patients suffering from post-infarction ventricular dysfunction in clinical trials [29, 30].

The FACS sorting gate was designed to encompass only the central 25% of the CD8 fluorescence intensity range of the reference clone because we found previously that restricting the sorting gate improved the precision of sorting for chosen VEGF levels and improved the safety of the induced angiogenesis. Cells purified with a gate corresponding to the full fluorescence range of the reference clone had led to rare instances of aberrant vascular structures in non-ischemic tissue, which were altogether avoided with a more restrictive gate, similar to the one used in this study [11]. Interestingly, we previously observed that an intermediate gate size, encompassing 50% of the reference clone fluorescence range, led to rare vascular structures with an only partially aberrant phenotype, characterized by irregular enlargement, and also by full maturation with normal pericytes and lack of angioma-forming potential in the long term [11]. The gate corresponding to the central 25% of the fluorescence range was designed to balance the aim of avoiding any aberrant vessel growth while still yielding sufficiently large numbers of cells. The gate appears 'shifted' towards the upper end of the reference clone range because the central 25% was calculated on a linear range (CD8 fluorescence and VEGF expression being correlated linearly, see Fig. 1d), whereas data in the FACS histogram are plotted on a logarithmic scale.

In summary, we found that FACS-purified VEGF-expressing myoblasts induced normal and long-term stable angiogenesis in chronically ischemic muscle. This approach affords control over VEGF expression at the microenvironmental level, which is a

prerequisite for the safety of therapeutic angiogenesis strategies. Dose-finding studies with increasing numbers of purified VEGF-expressing cells and implantation sites are now necessary in order to ensure treatment efficacy.

Acknowledgements

Conflict of interest

The authors confirm that there are no conflicts of interest.

References

1. **Carmeliet P.** Angiogenesis in health and disease. Nat Med. 2003; 9: 653–60.
2. **Yla-Herttuala S, Rissanen TT, Vajanto I, et al.** Vascular endothelial growth factors: biology and current status of clinical applications in cardiovascular medicine. *J Am Coll Cardiol.* 2007; 49: 1015–26.
3. **Schwarz ER, Speakman MT, Patterson M, et al.** Evaluation of the effects of intramyocardial injection of DNA expressing vascular endothelial growth factor (VEGF) in a myocardial infarction model in the rat–angiogenesis and angioma formation. *J Am Coll Cardiol.* 2000; 35: 1323–30.
4. **Carmeliet P.** VEGF gene therapy: stimulating angiogenesis or angioma-genesis? *Nat Med.* 2000; 6: 1102–3.
5. **Lee RJ, Springer ML, Blanco-Bose WE, et al.** VEGF gene delivery to myocardium: deleterious effects of unregulated expression. *Circulation.* 2000; 102: 898–901.
6. **Pettersson A, Nagy JA, Brown LF, et al.** Heterogeneity of the angiogenic response induced in different normal adult tissues by vascular permeability factor/vascular endothelial growth factor. *Lab Invest.* 2000; 80: 99–115.
7. **Springer ML, Chen AS, Kraft PE, et al.** VEGF gene delivery to muscle: potential role for vasculogenesis in adults. *Mol Cell.* 1998; 2: 549–58.
8. **Park JE, Keller GA, Ferrara N.** The vascular endothelial growth factor (VEGF) isoforms: differential deposition into the subepithelial extracellular matrix and bioactivity of extracellular matrix-bound VEGF. *Mol Biol Cell.* 1993; 4: 1317–6.
9. **Ozawa CR, Banfi A, Glazer NL, et al.** Microenvironmental VEGF concentration, not total dose, determines a threshold between normal and aberrant angiogenesis. *J Clin Invest.* 2004; 113: 516–27.
10. **von Degenfeld G, Banfi A, Springer ML, et al.** Microenvironmental VEGF distribution is critical for stable and functional vessel growth in ischemia. *FASEB J.* 2006; 20: 2657–9.
11. **Misteli H, Wolff T, Fuglistaler P, et al.** High-throughput flow cytometry purification of transduced progenitors expressing defined levels of vascular endothelial growth factor induces controlled angiogenesis *in vivo. Stem Cells.* 2010; 28: 611–9.
12. **Ghattas IR, Sanes JR, Majors JE.** The encephalomyocarditis virus internal ribosome entry site allows efficient coexpression of two genes from a recombinant provirus in cultured cells and in embryos. *Mol Cell Biol.* 1991; 11: 5848–59.
13. **Rando TA, Blau HM.** Primary mouse myoblast purification, characterization, and transplantation for cell-mediated gene therapy. *J Cell Biol.* 1994; 125: 1275–87.
14. **Springer ML, Blau HM.** High-efficiency retroviral infection of primary myoblasts. *Somat Cell Mol Genet.* 1997; 23: 203–9.
15. **Banfi A, Springer ML, Blau HM.** Myoblast-mediated gene transfer for therapeutic angiogenesis. *Methods Enzymol.* 2002; 346: 145–57.
16. **Prior BM, Lloyd PG, Ren J, et al.** Time course of changes in collateral blood flow and isolated vessel size and gene expression after femoral artery occlusion in rats. *Am J Physiol Heart Circ Physiol.* 2004; 287: H2434–47.
17. **Yang HT, Terjung RL.** Angiotensin-converting enzyme inhibition increases collateral-dependent muscle blood flow. *J Appl Physiol.* 1993; 75: 452–7.
18. **Laughlin MH, Armstrong RB, White J, et al.** A method for using microspheres to measure muscle blood flow in exercising rats. *J Appl Physiol.* 1982; 52: 1629–35.
19. **Mizuguchi H, Xu Z, Ishii-Watabe A, et al.** IRES-dependent second gene expression is significantly lower than cap-dependent first gene expression in a bicistronic vector. *Mol Ther.* 2000; 1: 376–82.
20. **Dor Y, Djonov V, Abramovitch R, et al.** Conditional switching of VEGF provides new insights into adult neovascularization and pro-angiogenic therapy. *EMBO J.* 2002; 21: 1939–47.
21. **Gussoni E, Blau HM, Kunkel LM.** The fate of individual myoblasts after transplantation into muscles of DMD patients. *Nat Med.* 1997; 3: 970–7.
22. **Heil M, Eitenmuller I, Schmitz-Rixen T, et al.** Arteriogenesis *versus* angiogenesis: similarities and differences. *J Cell Mol Med.* 2006; 10: 45–55.
23. **Eitenmuller I, Volger O, Kluge A, et al.** The range of adaptation by collateral vessels after femoral artery occlusion. *Circ Res.* 2006; 99: 656–62.
24. **Yla-Herttuala S, Markkanen JE, et al.** Gene therapy for ischemic cardiovascular diseases: some lessons learned from the first clinical trials. *Trends Cardiovasc Med.* 2004; 14: 295–300.
25. **Yla-Herttuala S.** An update on angiogenic gene therapy: vascular endothelial growth factor and other directions. *Curr Opin Mol Ther.* 2006; 8: 295–300.
26. **Kupatt C, Hinkel R, Pfosser A, et al.** Cotransfection of vascular endothelial

growth factor-A and platelet-derived growth factor-B *via* recombinant adeno-associated virus resolves chronic ischemic malperfusion role of vessel maturation. *J Am Coll Cardiol.* 2010; 56: 414–22.

27. **Marsh RL, Ellerby DJ.** Partitioning locomotor energy use among and within muscles. Muscle blood flow as a measure of muscle oxygen consumption. *J Exp Biol.* 2006; 209: 2385–94.

28. **Machida S, Spangenburg EE, Booth FW.** Primary rat muscle progenitor cells have decreased proliferation and myotube formation during passages. *Cell Prolif.* 2004; 37: 267–77.

29. **Menasche P, Hagege AA, Scorsin M, *et al*.** Myoblast transplantation for heart failure. *Lancet.* 2001; 357: 279–80.

30. **Menasche P, Hagege AA, Vilquin JT, *et al*.** Autologous skeletal myoblast transplantation for severe postinfarction left ventricular dysfunction. *J Am Coll Cardiol.* 2003; 41: 1078–83.